

Self-potential Anomalies Associated with Subsurface Electrokinetic and Electric Current Density Coupling in Parts of Southern Nigeria

**Evans Udoh Felix¹, Ayedun Funmilayo², Umoh Mfon David³
and Akpabio Idara Okon⁴**

Abstract

Self-potential (SP) anomalies due to electrokinetic and electric current density coupling were measured and analyzed with the aim of determining associated electrokinetic (EK) coupling coefficient induced by groundwater. The study deployed two non-polarizable Cu/CuSO₄ electrodes and high impedance volt meter (Metrix MX-20) connected via reel of insulated wire to measure the subsurface electrical potential anomalies in parts of Southern Nigeria particularly Ikot Umiang Ede catchment plain, Etinan LGA. SP measurements were performed along 4 profiles, where data were collected at sample intervals of 25.0m using total station approach. This was complemented by resistivity and geologic data obtained from VES and dug wells respectively. The result showed strong agreement with the local hydrogeological conditions of the environment. Low subsurface resistivity values were delineated at depth consistent with the local hydrostatics. Also, the amplitude of SP anomalies tends to be antisymmetric across the survey areas, with places of low resistivity values having weak magnitude potential anomalies. Similarly, places with high resistivity values showed strong amplitude potential anomalies. It was inferred that SP absolute potential anomaly provide information on groundwater flux of an area.

Keywords: Subsurface, Self-Potential Anomalies, Electrokinetic, Hydrostatic pressure, Groundwater flux.

¹ Directorate of Research and Strategic Development, Maritime Academy of Nigeria.

² Department of Pure and Applied Science, National Open University of Nigeria, Abuja.

³ Directorate of Research and Strategic Development, Maritime Academy of Nigeria.

⁴ Department of Geoscience, University of Uyo, Uyo.

1. Introduction

Water is a fundamental requirement for the survival of all living things. Potable water source can exist as surface water or underground water. However, not all water sources are suitable for use due to pollution from anthropogenic activities. The heavy pollution of water sources, especially the surface water, in the Niger Delta has caused residence to depend absolutely on groundwater for potable supply. Consequently, groundwater has become the main source of potable water for the entire population of the study area. The movement of groundwater require work done to overcome frictional force between water molecules and soil pore spaces. Therefore, as groundwater moves in the subsurface, it generates small electrical currents. These subsurface currents generate small voltage differences, which can be measured on the ground surface (Singh, 2014; Shapoori *et al.*, 2015; White *et al.*, 2016). The pores and fractures of underground materials such as sand, gravel, and other rocks may be filled with groundwater, which flow naturally out of rock materials, and can equally be abstracted by pumping from aquifers, (Akpabio and Eyeneka, 2008). The search for groundwater requires a good knowledge of subsurface layers, aquifers' location and thickness as well as the directions of water fluxes. These can be achieved with geophysical prospecting, principally by electrical prospecting, which self-potential method is one. Resistivity prospecting is used to extricate differences in electrical resistivity of surface layers. These differences can be interpreted in terms of change in soil texture and structure between water-bearing and waterproof layers, which form a framework for subsurface water fluxes, and has been extensively applied (Revil *et al.*, 2003; Evans *et al.*, 2012).

SP method is a passive geophysical method that is based on the natural occurrence of electrical field on the Earth's surface. SP is sensitive to water fluxes in saturated and partially saturated porous media, such as those associated with rainwater infiltration and groundwater recharge (Lampe, 2011; Evans *et al.*, 2014). Natural electrical field sources in the subsurface identifiable by SP can be generated by several physical and chemical phenomena. One of these phenomena include streaming (electrokinetic) potential, which has its source from fluid (such as groundwater) flow through a porous medium; rapid fluid disruption; thermoelectric processes and solvent of different minerals (Akpabio and Ekpo 2008). In the light of these sources, self-potential can be used in groundwater investigation, as well as in geotechnical engineering (primarily to determine ground seepage). Electrokinetic phenomenon is directly related to the existence of an electric double layer between subsurface fluid and rock matrix (Luong and Sprik, 2014). This phenomenon is produced as fluid percolates through the soil, which is driven by a pore pressure gradient.

This study seeks to determine associated electrokinetic coupling coefficient due to groundwater flow by correlating SP gradient with water fluxes in the study area. In general, electrokinetic (EK) process is a complex phenomenon, which occurs when water flows through a porous medium such as the soil (Corwin and Hoover, 1979;

Jouniaux and Pozzy, 1995; Hase *et al.*, 2003; Alzawa *et al.*, 2008; Jouniaux *et al.*, 2009; Lampe, 2011; Eppelbaum, 2021). Of all existing electrokinetic phenomena, streaming potential and seismoelectric effects play an important role in geophysical applications. For instance, seismoelectric and electroseismic effects are induced by seismic wave propagation, and are used to investigate oil and gas reservoirs, hydraulic reservoirs as well as downhole seismoelectric imaging (Jouniaux and Ishido, 2012). On the other hand, streaming potential is used to map subsurface flow and detect subsurface flow patterns especially in oil reservoirs (Revil *et al.*, 2006). Subsurface flow in geothermal and volcanoes in addition to groundwater flow system in sedimentary formations can be monitored using streaming potential (Goto *et al.*, 2012; Singh, 2014). Monitoring of streaming potential anomalies has been proposed as a means of forecasting earthquakes (Luong and Sprik, 2014; Zhang and Lu, 2022).

EK is affected by several key parameters including the chemical composition of groundwater and the zeta potential, which is the electrical expression of the interaction between ions along the Helmholtz double layer (Hase *et al.*, 2003; Okiwelu *et al.*, 2011; Zhang and Lu, 2022). The significant parameter for electrokinetic phenomenon is the streaming potential coupling coefficient, hence, the zeta potential. The coupling coefficients mainly depend on the fluid chemistry, conductivity and pH, and on rock properties. Li *et al.* (2016) studied the effects of surface conductivity on zeta potential of calcite, the result indicated that subsurface conductivity of porous media had influence on the zeta potential, which also was a function of subsurface electrokinetic distributions. Their study further revealed underestimation of zeta potential by Helmholtz-Smoluchowski equation when applied to calcite at low salinities. It became obvious that subsurface conductivity of the streaming potential coupling coefficient. This coefficient relates the fluid and streaming potential gradients when the total current density is zero.

The SP surveys are useful in localizing and quantifying water-bearing formation, directions and intensities groundwater fluxes, pollutant plume spreading, and for estimating pertinent hydraulic properties of aquifers (such as water table, hydraulic conductivity). In spite of the above, the application SP method in Akwa Ibom State and the entire South south of Nigeria has not been very popular. Therefore, SP anomalies due to electrokinetic and electrical current density coupling were used to determine associated electrokinetic coupling coefficient induced by groundwater flow. The coupling coefficient is efficient means of predicting the direction and intensity of groundwater fluxes.

1.1 Geology of the Study Area

The study area is in Akwa Ibom State, located in the coastal southern part of Nigeria, lies between latitudes 4°32'N and 5°33'N, and longitudes 7°25'E and 8°25'E. The geology is that of the deltaic depositional environment of the Niger Delta Basin; characterized by coastal plain sediments. The coastal nature of the study area makes it a natural deposit of mosaic of marine, deltaic, estuarine, lagoonal and fluvio-

lacustrine and clay materials. The aquifer system in the study area is predominantly confined multilayer system and consist of gravel and sandstone interbedded with siltstones, mudstones and shales (Reijers *et al.*, 1997; Aizawa *et al.*, 2008). The multilayer system of rock unit was formed over millions of years from the deposition and then the silicification of rock forming sediments in depressions. Therefore, alternating layers of clays, silts, sands and gravel occurred due to variation in the landscape over time with stream, rivers, floodplains and creeks forming at different stages. The sandy sediments consolidated to form the permeable sandstone aquifers and the clayey sediments consolidated to form the impermeable shales and mudstone. Generally, the subsurface has heterogeneous geologic formations, with significant portion having highly expansive deltaic marine clay of the Benin Formation.

1.2 The Physics of Self-Potential (SP)

Self-potential method relies basically on subsurface redox reaction occasioned by groundwater movement. This makes the earth materials behave like a natural battery responsible for current flows through the earth materials, with groundwater acting as the electrolyte. Therefore, the theory of SP involves spatial distribution of time-invariant natural electrical potential associated with subsurface fluid flow. At macroscopic scale, streaming potential for porous soil is of the linear irreversible thermodynamics, whose fluxes are linear function of the thermodynamic forces (Titov, 2005; Jinadasa and Silva, 2009; Yousef *et al.*, 2020). According to Ohm's law, electrical charge flux is proportional to electrical field; whereas by Darcy's law, hydraulic flux is proportional to pore water pressure gradient. Hence, groundwater flow induces subsurface electric field. This gives rise to cross-coupling process. It infers that, streaming potential can be expressed in terms of current density (j , in Am^{-2}) as well as hydrostatic pressure (p) respectively as:

$$j = -\sigma \nabla \phi - i \nabla p \quad (1)$$

$$p = \rho_w g (H - z) \quad (2)$$

where σ (Sm^{-1}) is the electrical conductivity, ϕ is the electrical potential (V), i is the current coupling coefficient ($\text{APa}^{-1} \text{m}^{-1}$), ρ_w is the water density (kg m^{-3}), g is the gravity acceleration (ms^{-2}), H is the hydraulic head (m) and z is the constant elevation (m) from which the hydraulic heads are measured. The first term of the right-hand side of eq. (1) represents the conduction current density (Ohm's law), while the second term corresponds to the streaming current density (source current). Provided the water density to be constant across a porous medium, eqs (1) and (2) can be combined to yield:

$$j = -\sigma \nabla \phi - L \nabla H \quad (3)$$

where L is the coupling term expressed in Am^{-2} .

It is the electrical current density produced per unit hydraulic gradient given by

$$L = jx \frac{dl}{dh} \quad (4)$$

By taking the ratio of L to the subsurface electrical conductivity (σ), we have voltage drop per unit hydraulic gradient called the potential coupling coefficient (Vm^{-1}).

$$C = -L/\sigma \quad (5)$$

The unit of potential coupling coefficient implies the slope of potential-distance plot.

At the quasi-static level the principle of charge conservative is applied as thus;

$$\nabla \cdot j = 0 \quad (6)$$

By combining eqs (3) and (6), the electrical potential can be written in the form of Poisson equation as:

$$\nabla \cdot (\sigma \nabla \phi) = -\nabla \cdot (L \nabla H) \quad (7)$$

Interestingly, diffusion equation governs groundwater flow (Bear) and it is given by

$$\nabla \cdot (k \nabla H) = S_s \frac{\partial H}{\partial t} + q \quad (8)$$

where k is the hydraulic conductivity (ms^{-1}), S_s is the specific storage (m^{-1}) and q represents hydraulic sources and sinks (s^{-1}). Combining eqs (7) and (8), we obtain equation (9), which contains the hydraulic (external) sources of the electric field at the right-hand side.

$$\nabla \cdot (\sigma \nabla \phi) = -L \left\{ \frac{q}{k} + \frac{S_s}{k} \frac{\partial H}{\partial t} + \nabla (InL - Ink) \cdot \nabla H \right\} \quad (9)$$

At groundwater pumping stage, the right-hand side of eq. (9) contains three types of the external sources; the first term corresponds to primary hydraulic sources and sinks. The second term specifies sources related to the compressibility of the porous sediments and is non-zero in regions of the transient groundwater flow. The third term describes secondary hydraulic sources produced by inhomogeneities in the current coupling coefficient and hydraulic conductivity, which are crossed by the groundwater flow (Bogosvsky et al., 1973; McDonald & Harbaugh, 1988; Press *et*

al., 1992; Allerge, *et al.*, 2014; Cerepi, *et al.*, 2017). At the shutdown of pump, the first term in eq. (9) vanishes, and hydraulic sources related to the compressibility and inhomogeneities are responsible for the streaming potential response to the relaxation of hydraulic heads given as,

$$\nabla \cdot (\sigma \nabla \varphi) = -L \left\{ \frac{s_s}{k} \frac{\partial H}{\partial t} + \nabla (InL - Ink) \cdot \nabla H \right\} \quad (10)$$

During pumping, hydraulic heads decrease and the section of the aquifer from which water is pumped becomes unsaturated. The unsaturated aquifer section becomes inactive when the hydraulic head decreases up to the aquifers' bottom. When the pump is shutdown, hydraulic heads increase, and an inactive aquifer's section becomes active restored aquifers (Revil *et al.*, 2006; Eppelbaum, 2021). This is of interest because the main component of streaming potential anomalies is the friction between flow volume of groundwater and the soil particles.

2. Preliminary Notes

The instruments used for measuring subsurface streaming potential were two non-polarizable Cu/CuSO₄ electrodes (porous pots), high impedance volt meter (Metrix MX-20, with accuracy of 1mV) and a reel of abrasion-resistant insulated wire (about 1600m) for field work. The non-polarizable electrodes were connected to the millivolt meter via the insulated reel of wire and used to measure the subsurface self-potential anomalies along profile lines at *Ikot Umiang Ede* catchment plain, Etinan LGA, Akwa Ibom State, Nigeria. The porous pots were sealed to protect the salt solution (Cu/CuSO₄) from evaporation, therefore maintaining super-saturation of the porous pots' solutions for days. The nonpolarizing electrodes were preferred to steel electrodes because the nonpolarizing electrodes produce very low electrolytic contact potential, which rendered the background voltage negotiable. In addition, the steel electrodes often have quite high contact potentials, which varies in the soil at different locations due to polarization of the steel electrodes. Besides, avoiding the use of steel electrodes during SP data collection as a precautionary measure to prevent polarization, porous pots were refilled 24 hours before use for data collection. This was done to minimise the possibility contact potential change while performing a measurement. The mixing of the fluid was done in a single container and solution was well mixed to achieve homogenous solution before filling the pots. In addition, the Base station pot was larger in size to ensure constant electrical contact throughout the time of use of that station, while the mobile or traveling or roving pot had a smaller volume of salt solution. The wire used for the survey was strong, hardy, and of low resistance. In addition, the wire was of sufficient tensile strength to withstand long-term pulls during survey work. Therefore, a wire of constant resistance was used to acquire data.

The fixed-base configuration for self-potential mapping was used because of its low level of cumulative error and the greater efficiency as well as its associated speed, which are obtainable in the gradient configuration. The normal voltage, reverse

voltage and the contact resistance were measured at each station. The normal voltage was measured with the base electrode connected to the negative terminal of the voltmeter, and the roving electrode to the positive terminal by convention. Conversely, the reverse voltage was measured by reversing the polarity voltmeter. This was done to check if there was any problem with the circuit. The contact resistance was measured to determine if the circuit was complete and to ensure that there was no interference. SP data were obtained along profiles A-A', B-B', C-C' and D-D' (Figure 1) established in the study area. These profiles were chosen to minimize interference from cultural installations, in order to optimize data validity and reliability as well as the number of subsurface features intersected. The Base-electrode was fixed to the ground at the Base-station, while the second pot was a Roving electrode, which was moved along the profiles. However, a third non-polarizable electrode (called the Reference electrode) was deployed and allowed to stay permanently in the bucket of solution for adjusting for drift of the roving electrode with respect to the base electrode. It was assumed that the potential between the base and reference electrodes remained constant, hence, this additional electrode aided computation and adjustment for drift. Therefore, intermediate drift correction values were obtained by periodically reading the potential between the Roving and the Reference electrodes carried in the solution. In addition, the first reading on the SP profile was repeated at the end of each day to establish total daily drift. Hence, observed consistent drift difference between the base and roving pots was corrected to obtain absolute SP anomalies. Data were collected with the assumption that the roving electrode was planted at the vertex of a 120° cone, to increase depth of investigation (equation 11). Evans *et al.* (2012) relate the base diameter (Φ) of a 120° cone to the depth of investigation using Cu/CuSO₄ electrodes by:

$$d = \frac{\Phi}{2\sqrt{3}} \quad (11)$$

where d is the estimated depth of penetration interest, and the base-diameter (Φ) represents the electrodes spacing. A total of 95 SP anomalies were manually digitized at sampling intervals of 25.0m along four profiles. Complementary data for the study were subsurface resistivity and site lithology log obtained from VES and dug wells respectively.

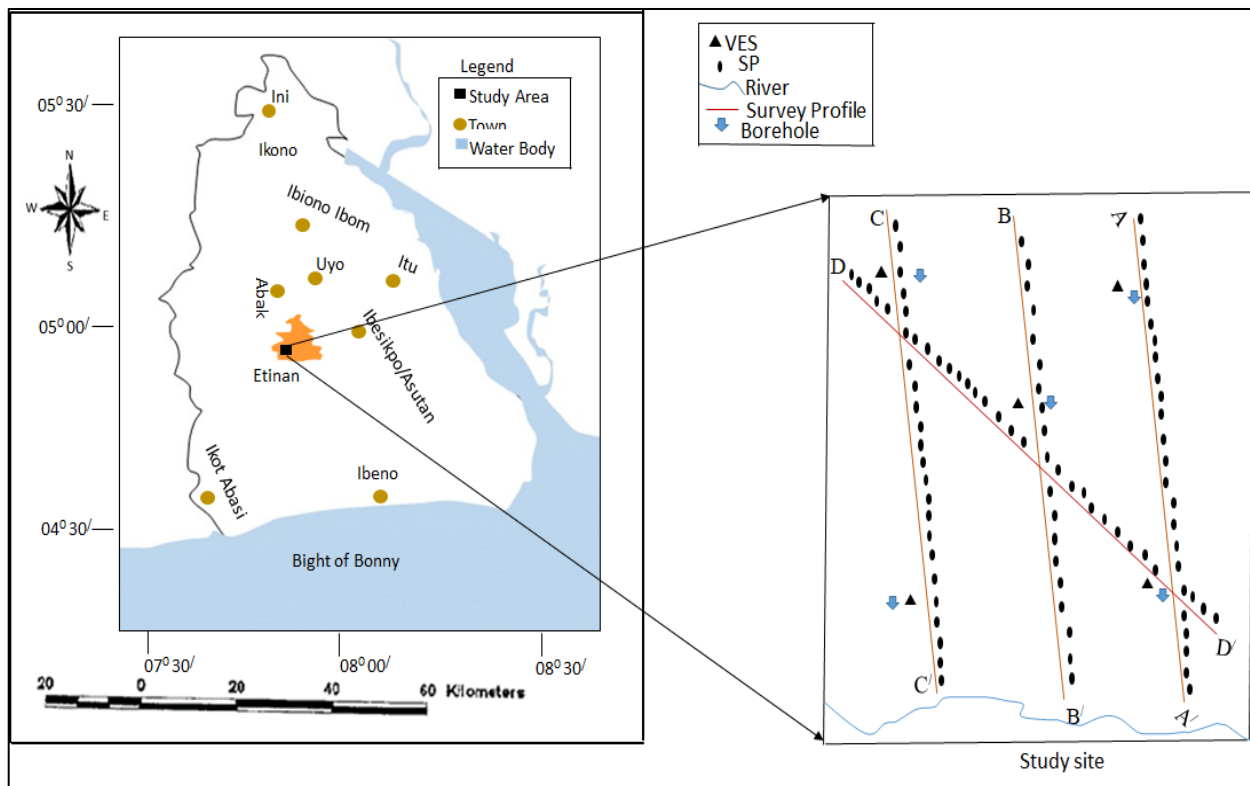


Figure 1: Map of Etinan Local Government Area showing SP survey points

SP data obtained were processed to obtain the absolute voltage for each profile. The absolute voltage obtained was plotted against electrode spacing to obtain SP signals. The moving three-point average technique was applied to the field data obtained. The SP investigations use a qualitative evaluation of the profile amplitudes or grid contours to evaluate self-and streaming-potential anomalies. To ensure control, ground resistivity and lithology log data were elucidated from VES and dung wells respectively. The VES data obtained from four locations were modelled using IPI2WIN.

3. Results and Discussion

Results obtained from modelled VES data are presented in Figure 2. This was compared with the hydrogeological data from dung wells. The results indicate shallow aquifers with undulating groundwater table laying at average depth of 1.0m. The shallow buried of groundwater was inferred to be responsible for the drop in resistivity (as low as $16.6\Omega\text{m}$) of the second layer at VES 2. The local lithology obtained from drilled wells near VES 1, VES 2 and VES 3 showed brownish-greyish coloured moist fine-grained sands.

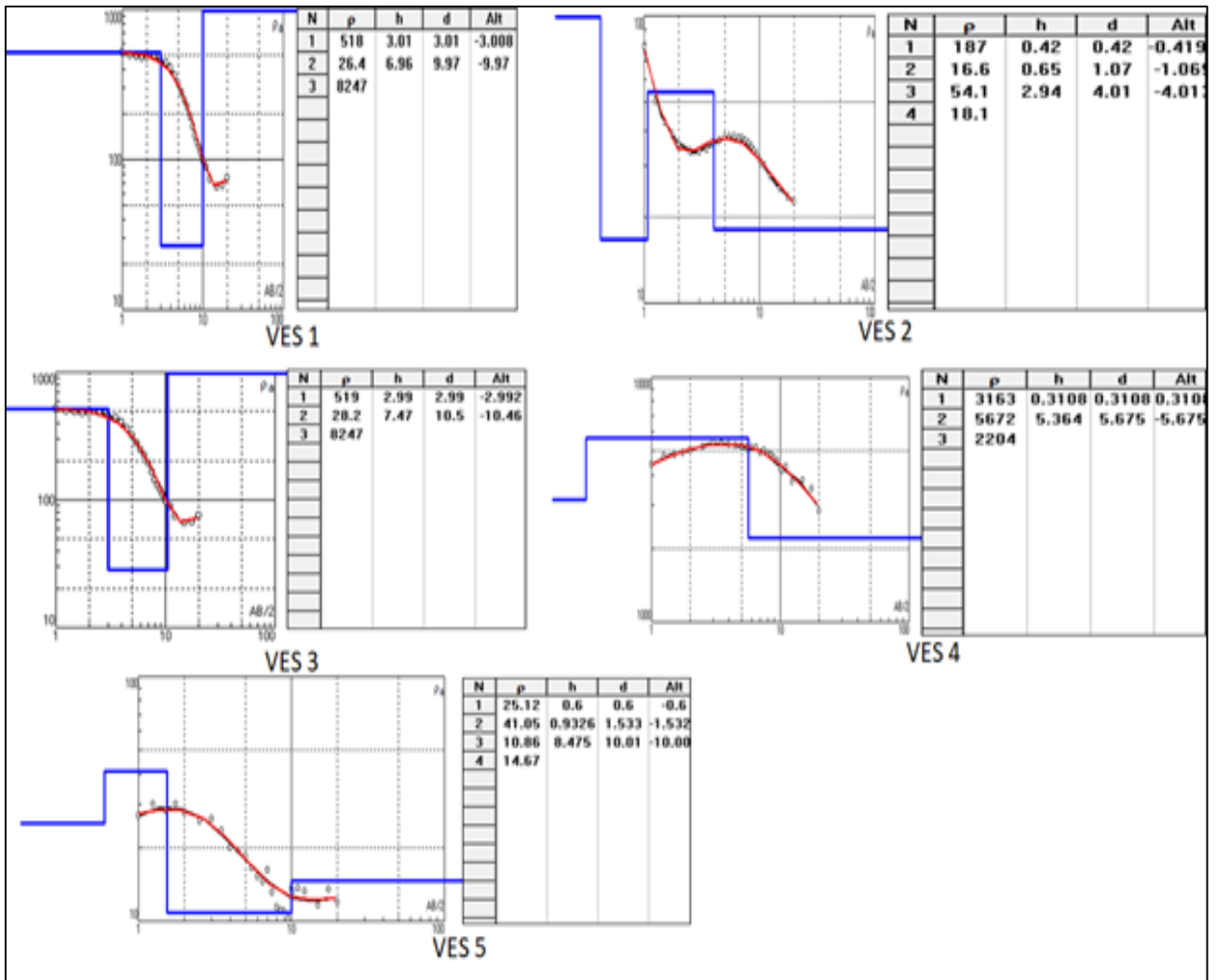


Figure 2: Results for VES in data interpreted for the study area

The spatial distributions of SP data along chosen profiles is the qualitative presentation of SP results (Figure 3). It is the plots of absolute SP anomalies against electrode spacing for each profile. This qualitative interpretation of SP indicates closely related patterns of SP anomalies over the study area. Profile A-A' indicates a maximum positive anomalies potential of 19mV within electrode spacing of 250m from the fixed electrode. However, the maximum negative anomaly of -20mV was observed at 90m from the fixed electrode.

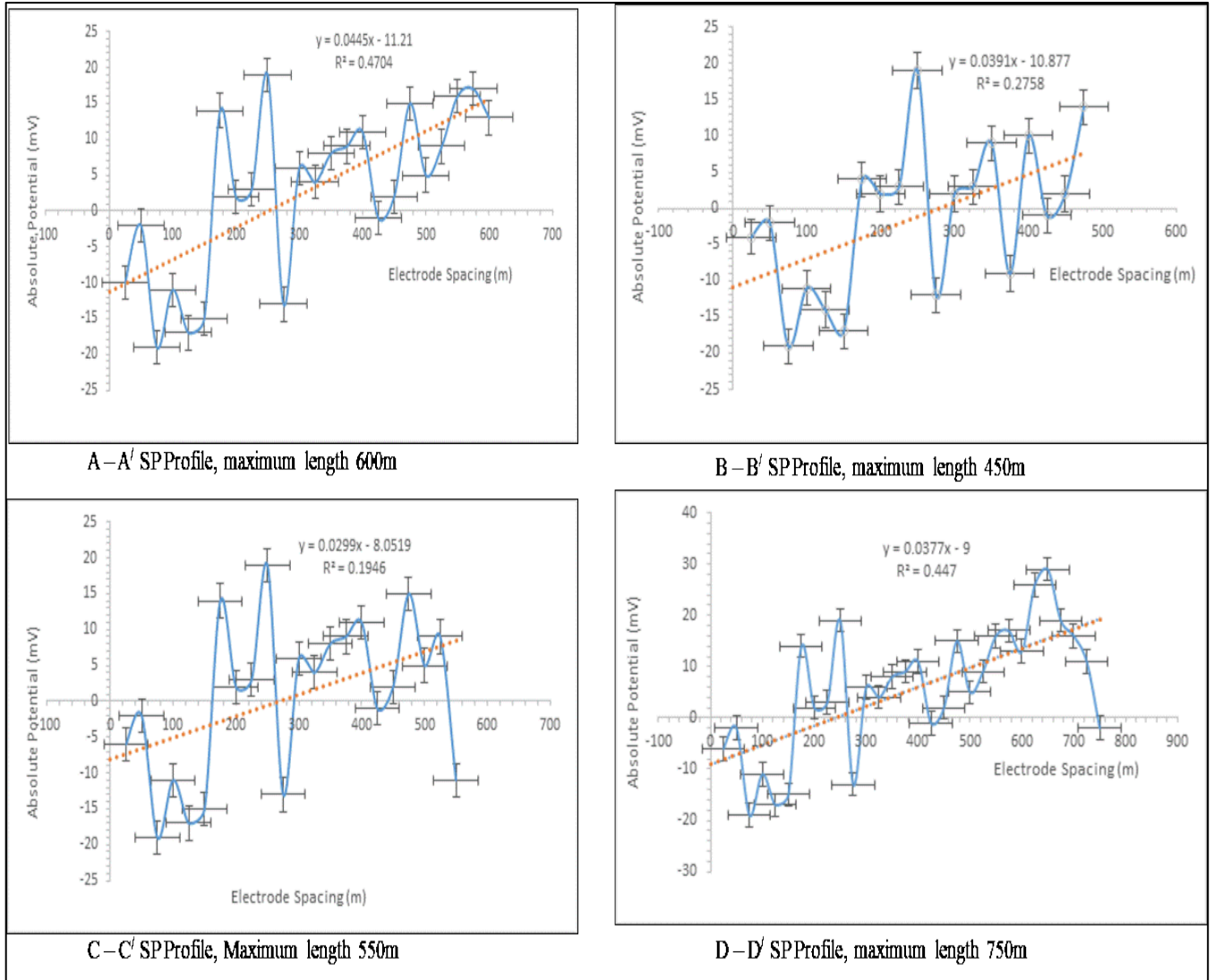


Figure 3: SP Anomalies for the Profiles for the study area

The plot indicates a large amount of positive SP anomaly variability between 300m - 600m. A potential coupling coefficient of 0.044 was obtained. This anomaly was observed across sandy-clay formation of the survey profile A-A' as revealed by the well along the profile. This anomaly represents a greater influence of electrochemical effect of the nearby streams at this survey line. The upper sections of all the SP profiles showed stronger amplitude anomalies. This corresponds to area of relatively higher subsurface resistivities of $6672\Omega\text{m}$ and $41.85\Omega\text{m}$ observed at VES 4 and VES 5 respectively within the established depth of groundwater table of about 1.2m. However, at the profiles end (A', B', C' and D') closer the stream showed lower amplitude anomalies, and they correspond to the observed lower resistivity zone mapped by VES1, VES2 and VES3 with resistivity values of

26.4 Ω m, 16.4 Ω m and 28.6 Ω m respectively. The width of the half-amplitude provides depth estimate for the SP survey, which the quantitative interpretation of current electrode spacing for VES survey provided the depth of investigation. Studies (Evans *et al.*, 2017; Cherubini *et al.*, 2018) have reveal that the depth of current penetration is usually less than 1/3 of half current electrode separation. This has also been confirmed by the depth delineated in the presented study. The 3D network spatial distribution of SP and VES results is shown in Figure 4. VES locations with low resistivity corresponds to weak SP anomalies area. Such as obtained in VES2. Locations with relatively higher resistivity are associated with higher values of SP anomalies.

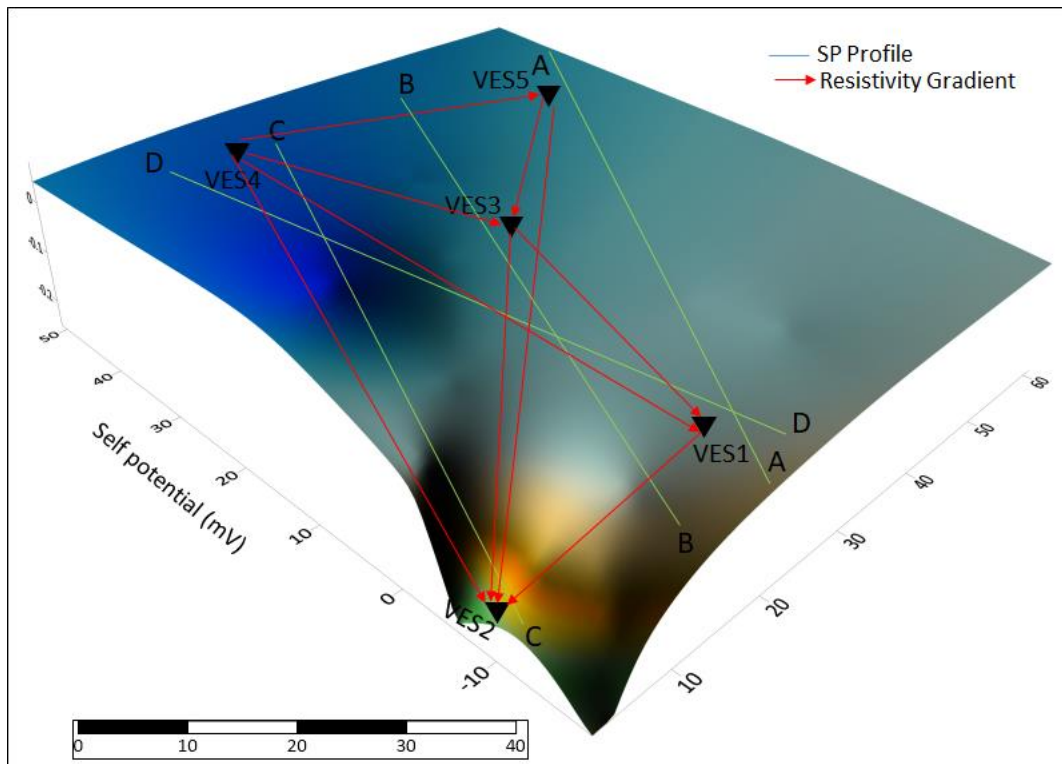


Figure 4: Spatial distribution of VES with SP data for the study area

Ultimately, the SP anomalies pattern indicates positive and negative polarity of varying amplitudes. The negative anomaly reading is likely caused by oxidation at the subsurface, which is created through oxygen-rich groundwater percolating downward. This causes a difference in polarity of subsurface layer, which create what is essentially a huge but weak battery in the earth. Therefore, the profile shape, amplitude, polarity and contour pattern were the basis for data interpretation. Hence, the subsurface of the study area was classified into positive and negative value anomalies. The positive SP anomalies such as observed in study is inferred to be

due to the local streams, which produces a positive current source near the ground surface. This is because, the *Esuk Ede* (stream) axis of the study area is widely covered by debris, which consist of unconsolidated sediments usually of high permeability. It is common to have perched water flow in a vadose zone developed in this location; therefore, it was inferred that the observed local SP anomalies reflect discharge of perched water, which emptied into the tributary of the Qua River at *Esuk Ede in Ikot Umiang Ede*.

The areas of negative values of the electrokinetic anomaly show that, positive ions are carried in the groundwater flow direction, and it indicates the presence of groundwater. It has earlier been explained by Li *et al.* (2016) that, in a water-saturated porous soil, there is always an excess of electrical charge located in the vicinity of the pore water mineral interface. The drag of excess of charge by the flow of groundwater is responsible for the net electrical current conduction. This is contrary to the positive values anomaly observed in some areas, which were interpreted to mean the presence of negative ions in the subsurface. Such areas could likely indicate the presences of hydrothermal zone. The region within zero electrokinetic coefficients was interpreted to mean that, the groundwater flow direction is free of contaminant sufficient enough to modify the ground electrokinetic coefficients. According to Goto *et al.* (2012), the lower the electrokinetic potential coupling coefficient of an area, the higher the groundwater flux.

The linear regression of electrokinetic coupling coefficient and absolute potential shows significant correlation with p-value < 0.05 alpha level (Table 1). The strength of prediction of electrokinetic coupling coefficient from absolute potential was 0.65. In addition, the extent to with absolute potential can predict electrokinetic coupling coefficient is about 62%. Since electrokinetic coupling coefficients is intrinsically related to groundwater (Cherubini *et al.*, 2018), it implies that the absolute potential can equally provide information on local groundwater potential of an area.

Table 1: Prediction of Electrokinetic Coupling from Absolute SP data

Model	R	R Square	Adjusted R Square	Std. Error of the Estimate	Change Statistics				
					R Square Change	F Change	df1	df2	Sig. F Change
1	.647 ^a	.619	.609	.045809829	.619	41.803	1	58	.000
a. Predictors: (Constant), AVSP									
b. Dependent Variable: EKCC									

4. Conclusion

The interpretation of SP signals is underlined by proper understanding of the main physical process involved in their origin. Self-potential (SP) measurements were conducted at Ikot Umiang Ede, Etinan, which is a sedimentary terrain forming part of the deltaic depositional environment, to infer groundwater flow system in the area. The reliability of observed SP anomaly was checked by using SP values along parallel survey routes; the error was almost within 10 mV. The field survey deployed total station to measure self-potential anomalies due to electrokinetic and electrical current density couplings along two profile lines. Complementary data were obtained from electrical resistivity soundings and drilled wells within the study area, which produce strong correlation with SP data. The measured absolute potential as well as the hydro pressure was used to provide better quantification of the electrokinetic coupling coefficients. The regression of measured absolute potential showed that, electrokinetic coupling coefficients can be predicted measured absolute potential for the study. Electrokinetic coupling coefficients is an intrinsic function of for predicting groundwater flux. This was there inferred that, Electrokinetic coupling in the study area is originated from the flow of an electrolyte (water) over naturally charged solids, and the study area has potential of providing potable groundwater supply at depth estimated using half width of the anomaly's amplitude along profiles.

Conflict of Interests: The Author declare no conflict of interest.

Disclosures and declarations: This work was funded through the selfless contribution by the authors. We disclose that, no external body supported in funding the work.

References

- [1] Aizawa, K., Uyeshima, M. Nogami, K. (2008). Zeta potential estimation of volcanic rocks on Island arc-type volcanoes in Japan: Implication for the generation of local self-potential anomalies. *Journal of Geophysical Research*, 113: DOI:10102912007JB005058
- [2] Allegre, V., Mainault, A., Lehmann, F., Lopes, F. and Zamora, M. (2014). Self-potential response to drainage–imbibition cycles. *Geophysical Journal International*, 197 (3), 1410–1424.
- [3] Akpabio I. O and Eyeneka, F. (2008), Aquifer Transmissivity Determination using Geoelectric Sounding data at Uyo, Southern part of Nigeria, *Scientia Africana*, 7 (1), 81-90, Nigeria
- [4] Akpabio I. O and Ekpo, E (2008) Geoelectric Investigation for Groundwater Development of Southern Part of Nigeria. *The Pacific Journal of Science and Technology*, 9 (1) 219 –226, USA. <http://www.akamaiuniversity.us/PJST.htm>
- [5] Bogoslovsky, V. V. and Ogilvy, A. A. (1973). Deformations of natural electric fields near drainage structure. *Geophysical Prospecting*, 12, 716-723.

- [6] Cerepi, A. Cherubini, A., Garcia, B., Deschamps, H. and Revil, A. (2017). Streaming potential coupling coefficient in unsaturated carbonate rocks. *Geophysical Journal International*, 210(1), 291-302.
- [7] Cherubini, A., Garcia, B., Cerepi, A. and Revil, R. (2018). Streaming Potential Coupling Coefficient and Transport Properties of Unsaturated Carbonate Rocks. *Vadose Zone Journal- Original Research*, 17 (1), 1-12.
- [8] Corwin, R. F. and Hoover, D. B. (1979). The self-potential method in geothermal exploration. *Geophysics*, 44, 226-245.
- [9] Eppelbaum, L. V. (2021). Review of processing and interpretation of self-potential anomalies: Transfer of methodologies developed in magnetic prospecting. *Geosciences*, 11(5),
- [10] Evans, U. F., Okiwelu, A. A., Ude, I. A. and Abima, J. O. (2012). Estimate of corrosion induced flow sizes on buried gas pipeline in the Nigerian sector of Niger Delta. *Research Journal of Environmental and Earth Science*, 4(3), 264-268.
- [11] Evans, U. F., Asamudo, N. U. and Ekanem, C. H. (2014). Proportionate risk-based approach to groundwater quality sustainability in the Nigerian Niger Delta. *Journal of Environment and Earth Sciences*, 14(12), 43-48.
- [12] Evans, U. F., Abdulsalam, N. N. and Mallam, A. (2017). Natural vulnerability estimate of groundwater resources in the coastal area of Ibaka community using Dar Zarrouk geoelectrical parameters. *Journal Geology and Geophysics*, 6, (4). DOI: 10.4172/2381- 8719.1000295
- [13] Goto, T., Kondo, K., Ito, R., Esaki, K., Oouchi, Y., Abe, Y. and Tsujimura, M. (2012). Implications of self-potential distribution for groundwater flow System in a Nonvolcanic Mountain Slope. *International Journal of Geophysics*.
- [14] Jinadasa, S. and Silva, R. (2009). Resistivity imaging and self-potential applications in groundwater investigations in hard crystalline rocks. *Journal of the National Science Foundation of Sri Lanka*, 37(1), 23-32.
- [15] Jouniaux, L. and Naudet, V. (2009). Review of self-potential methods in hydrogeophysics. *Comptes Rendus Geosciences*, 341(10). DOI: 10.1016/j.crte.2009.08.008.
- [16] Jouniaux, L and Ishido, T. (2012). Electrokinetics in Earth Sciences: A Tutorial. *International Journal of Geophysics*. <http://dx.doi.org/10.1155/2012/286107>.
- [17] Lampe, R. J. (2011). Monitoring Groundwater Flow using Electrokinetics. Thesis, School of Physical Sciences. <https://hdl.handle.net/2440/96682>.
- [18] Luong, D. T. and Sprik, R. (2014). Examination of a Theoretical Model of Streaming Potential Coupling Coefficient.
- [19] Li, S., Leroy, P., Heberling, F., Devau, N., Jougnot, D. and Chiaberge, C. (2016). Influence of surface conductivity on the apparent zeta potential of calcite. *Journal of Colloid Interface Science*, 468, 262–275.
- [20] Okiwelu, A., Evans, U. and Obianwu, V. (2011). Geoelectrical investigation of external corrosion of earth buried pipeline in the coastal area of Gulf of Guinea. *Journal of American Sciences*, 7(8), 221-226.

- [21] Reijers, T. J. A., Petters, S.W., Nwajide, C. S. (1997). The Niger Delta Basin, in Selley, R.C., ed., *African Basins-Sedimentary Basin of the World 3*: Amsterdam, Elsevier Science, pp.151- 172.
- [22] Revil, A., Titov, K., Doussan, C. and Lapenna, V. (2006). Applications of the self-potential method to hydrological problems. *Applied Hydrogeophysics*, 71, 255-292.
- [23] Revil, A. and Mahardika, H. (2013). Coupled hydromechanical and electromagnetic disturbances in unsaturated porous materials. *Water Resource*, 49. doi:10.1002/wrcr.20092.
- [24] Revil, A. Naudet, V. Nouzaret, J. Pessel, M. (2003). Principles of electrograph applied to self-potential electrokinetic sources and hydrogeological applications. *Water Resources Research*, 39 (5), 426-542.
- [25] Yousef, S. B. A., Yousef, M. H. M., Abd-Elsalam, H. F. and Shaheen, M. A. M. (2020). Detection of the possible buried archeological target using the Geophysical methods of ground penetrating radar and self-potential, Kom Ombo Temple, Aswan Governorate, Egypt. *Geomaterials*,10,4. DOI:10.4236/gm.2020.104007.
- [26] Shapoori, V., Peterson, T., Western, A. and Costelloe, J. (2015). Top-down groundwater hydrograph time-series modeling for climate-pumping decomposition, *Hydrogeology. Journal*, 23(4), 819– 836.
- [27] Singh, A. (2014). Groundwater resources management through the applications of simulation modeling: A review. *Science Total Environment*, 499, 414– 423.
- [28] Titov, K., Revil, A., Konosavsky, P., Straface, S. and Troisi, S. (2005). Numerical modelling of Self-potential signals associated with pumping test experiment. *Geophysical Journal International*, 162(2), 641-650.
- [29] White, E. K., Peterson, T. J., Costelloe, J., Western, A. W. and Carrara, E. (2016). Can we manage groundwater? A method to determine the quantitative testability of groundwater management plans. *Journal of Water Resources*, 52 (6), 4863-4882.
- [30] Zhang, L. and Lu, H. (2022). Investigation method and utilization mode of geothermal resource in abandoned mines in Human and Huaibei. *International Journal of Geosciences*, 13,6, DOI:10.4236/ijg.2022.136022.